LAWRENCE
LIVERMORE
NATIONAL
LABORATORY

LLNL-JRNL-773024

Hydrogen and Oxygen Stable Isotope Composition of Water in Metaschoepite Mineralization on U3O8

E. Oerter, M. Singleton, Z. Dai, A. Deinhart, M. Thaw, M. L. Davisson

April 26, 2019

Geochimica et Cosmochemica Acta

Disclaimer

Hydrogen and Oxygen Stable Isotope Composition of Water in Metaschoepite Mineralization on U_3O_8

Erik J. Oerter[1]*, Michael Singleton[1], Zurong Dai[1],
Amanda Deinhart[1], Melissa Thaw[1,2], M. Lee Davisson[1]

[1] Lawrence Livermore National Laboratory, 7000 East Avenue, Livermore, CA 94550, USA.
[2] University of California, Merced, 5200 Lake Road, Merced, CA 95340, USA.

* Corresponding Author email: oerter1@LLNL.gov

Highlights

We exposed U_3O_8 to air with constant relative humidity and known hydrogen and oxygen stable isotope composition of the water vapor for two periods of 90 days.

We measured the stable isotopes of hydration water in metaschoepite that formed on the U_3O_8.

$\delta^{18}O$ values of the metaschoepite hydration water are likely to reflect that of the water vapor the sample was exposed to.

It may be possible to discern information about the provenance and history of an oxidized U_3O_8 sample from oxygen stable isotope measurements of metaschoepite mineral hydration water.

Key Words

Mineral hydration water, humidity exposure experiments, nuclear forensics, stable isotope hydrology, isotope exchange

Abstract

When exposed to humidity in an oxidizing atmosphere hydrated uranium oxide grows as a secondary mineral on aged U_3O_8 and may incorporate the oxygen stable isotope signature of the water vapor into the secondary uranium oxide, as well as hydrogen and oxygen stable isotopes into any mineral hydration water. Because geospatial variation in δ^2H and $\delta^{18}O$ values of atmospheric humidity and precipitation is well understood, the H and O stable isotope composition of mineral hydration waters can give information on the environment of mineral formation. We exposed powdered U_3O_8 to humidity with known H and O stable isotope composition at constant 30%, 61% and 91% relative humidity. We sampled and analyzed the U_3O_8 powders along with any secondary hydrated minerals that had formed on the particle surfaces at various intervals from 1 to 10 days throughout the 180-day humidity exposures. We present stable H and O isotope results of mineral hydration waters in uranium oxide materials

analyzed by thermogravimetry-enabled isotope ratio infrared spectroscopy (TGA-IRIS), which uses precise heating by thermogravimetric analyzer to liberate water vapor for subsequent online isotope analysis via a laser-based isotope ratio infrared spectroscopy instrument (Picarro L-2130i). Scanning electron microscopy (SEM), transmission electron microscopy (TEM), and x-ray diffraction (XRD) analysis of humidity-exposed U_3O_8 heating to 350 °C indicates that the U_3O_8 had a measurable metaschoepite ($(UO_3)•2H_2O$) phase along with α-U_3O_8. After heating to 350 °C, the metaschoepite is eliminated but the α-U_3O_8 is retained, meaning that the heating successfully extracted the water in the metaschoepite but did not disturb the crystalline structure of the U_3O_8. Analysis of the bulk oxygen isotope composition by fluorination of these samples before and after heating, indicates that the oxygen isotope value of the U_3O_8 is also not affected by heating to 350 °C. Precision for δ^2H and $\delta^{18}O$ values of metaschoepite mineral hydration water stable isotope values yielded by the TGA-IRIS method on metaschoepite are 5.86‰ for δ^2H, and 0.34‰ for $\delta^{18}O$. Hydrogen in the various water reservoirs is highly exchangeable and thus the δ^2H values of these waters is not easily interpreted. However, oxygen in the separate water reservoirs is much less exchangeable, and thus $\delta^{18}O$ values of the metaschoepite interlayer water is likely to reflect that of the water vapor the sample was exposed to. Once metaschoepite is formed on the surface of U_3O_8 particles, the oxygen isotope signature of the interlayer water in metaschoepite does not respond to changes in exposure vapor isotopic composition, and thus appears to be fairly durable in this regard. These results suggest that it may be possible to discern information about the provenance and history of an oxidized U_3O_8 sample from oxygen stable isotope measurements of metaschoepite mineral hydration water.

1. Introduction

The need for the development of techniques to determine the provenance and history of nuclear materials has been identified (Moody et al., 2005; Mayer et al., 2012) and many recent efforts have focused on radioisotopic and elemental approaches (e.g. Eppich et al., 2013; Keegan et al., 2014; Horne et al., 2014). U_3O_8 is ubiquitous in the production of nuclear material, and one potentially attractive approach that has not yet been developed to determine the provenance and history of U_3O_8 is the analysis of the hydrogen and oxygen stable isotope composition of hydrated uranium oxidation weathering products that form from it. Hydrated mineral weathering products are common in general, and form from exposure to oxidative conditions in the environment due to an abundance of water and oxygen at ambient temperatures (e.g. Garrels and Christ, 1965; Maher and Chamberlain, 2014).

Hydrated secondary minerals formed on U_3O_8 are also common (Tamasi et al., 2015; Lloyd et al., 2009; He et al., 2012) and many are included in the "schoepite group", with general formulae of $UO_3•xH_2O$ (Finch et al., 1992; Finch et al., 1996; Finch et al., 1998; Kubatko et al., 2006). Herein, we consider metaschoepite as $UO_3•2H_2O$ (Tamasi et al., 2015). The mineral crystal structure of the schoepite group is orthorhombic with an arrangement of planar uranyl sheets interleaved with water molecules in the interlayer spaces (Finch et al., 1996; Plasil, 2018). The structural difference between schoepite and metaschoepite is much smaller than previously considered, leading to the easy transformation of schoepite to metaschoepite under ambient conditions and a joint occurrence of both minerals (Plasil, 2018). Because these hydrated minerals form in response to the oxygen and water they are exposed to, that water may be retained in the mineral crystal structure (Lawrence and Taylor, 1971; 1972). In this way they may develop and retain information on the environmental conditions of their formation because

the parent water involved in the oxidation reactions may be of meteoric or ambient humidity origin, and therefore have geographically distinct hydrogen and oxygen stable isotope compositions (δ^2H and $\delta^{18}O$ values, defined below) (e.g. Dansgaard, 1964; Bowen, 2010). If the isotopic composition of this mineral hydration water can be measured, information about the mineral formation environment can be understood (e.g. Savin and Epstein, 1970; Shepard and Gilg, 1996; Savin and Hsieh, 1998).

Until the recent advent of thermogravimetry-enabled isotope ratio infrared spectroscopy (TGA-IRIS; Oerter et al., 2017) the isotopic analysis of mineral hydration water was restricted by the labor-intensive off-line water extraction and gaseous conversion required by conventional magnetic sector mass spectrometry. In the case of isotope ratio infrared spectroscopy, isotope ratio measurements are made by the differential laser absorption of the heavy (ex. ^2H) and light (^1H) isotopologues of water vapor (with no gaseous conversion) that the laser pulse encounters. TGA-IRIS is an attractive analysis method because with minimal sample preparation, the sample can be step-heated very precisely to release waters held in the mineral matrix at different binding strengths (i.e. lower temperatures for weakly-bound, higher temperature for strongly-bound), and the corresponding mass loss of each water type can be precisely measured. Thus, TGA-IRIS allows for the rapid on-line analysis of large numbers of samples for simultaneous measurements of water content, δ^2H and $\delta^{18}O$ values. In the case of U_3O_8 secondary mineralization, as well as other minerals that contain multiple reservoirs of oxygen and/or hydrogen, TGA-IRIS offers the additional possibility to isotopically measure only the hydrous reservoirs and leave the oxygen in the mineral crystal structure unaltered.

In this study, we exposed U_3O_8 to air with known water vapor content (relative humidity) and known hydrogen and oxygen stable isotope composition for two periods of 90 days. We periodically sampled the U_3O_8 through the exposure experiments and analyzed the secondary mineralization hydration water's hydrogen and oxygen stable isotope composition by TGA-IRIS. The purposes of this study were to: 1) determine the feasibility and precision of TGA-IRIS measurements of mineral hydration water in secondary mineralization of U_3O_8, 2) determine the effects of differing levels of water vapor (relative humidity levels) on the mineral hydration water accumulation rates of U_3O_8 secondary mineralization, 3) determine the effects of differing levels of water vapor (relative humidity levels) on the δ^2H and $\delta^{18}O$ values of mineral hydration water in U_3O_8 secondary mineralization, and 4) determine the extent to which the isotopic composition of U_3O_8 secondary mineralization hydration waters are maintained after initial formation.

2. Experimental Methods

2.1 Uranium material

A stock of powdered U_3O_8 (0.83 weight % ^{235}U) was obtained from New Brunswick Laboratory (Chicago, IL, USA). Mineral composition of the U_3O_8 material before and after the humidity exposure experiments were determined by X-ray diffraction on a Bruker D8 Advance instrument (Bruker Corp., Billerica, MA, USA) using Cu-Kα radiation generated at 40 kV and 40 mA. Diffraction scans were performed from 10-80° 2θ, with 0.02° 2θ step size with 2 sec collection time per step, with variable divergence slits.

2.2 Humidity Exposure Experiments

Three separate humidity exposure chambers were set up to create air with constant relative humidity (30%, 61%, 91%; ± 1.3%) and constant hydrogen and oxygen stable isotope composition of the water vapor (δ^2H_{vap}, ± 1.2‰; and $\delta^{18}O_{vap}$, ± 0.15‰). Aqueous salt-saturated solutions to control humidity were not used to avoid the deleterious effects that salts have on the resulting water vapor (Oerter et al., 2018). The conceptual design of the humidity exposure chambers is based on mixing of wet and dry air streams, and more detail can be found in Oerter et al. (2019). Briefly, a stream of dry air is directed to a water reservoir where it passes through a water vapor-permeable membrane immersed in the water. This water vapor-saturated air stream is then joined by a diluter stream of dry air before the combined stream enters the humidity chamber. The relative proportion of vapor and diluter air streams are adjusted via mass flow controllers to achieve the desired humidity level inside each chamber, which are 10.5 L in volume. Temperature and relative humidity (RH) inside the chambers are monitored by high precision digital thermometer and hygrometer (± 0.2 °C, ± <1% RH; HMT-330, Vaisala Inc., Finland), and relative humidity (RH) data are reported here. Each chamber received a total air flow of 500 standard cubic centimeters per minute (SCCM), corresponding to 3 air changes per hour, an air flow rate that is designed to emulate that of a typical warehouse ventilation system (ANSI, 2013). Two isotopically-distinct waters were used to supply water vapor: TWW with δ^2H_{liq} = -111.32 ‰ and $\delta^{18}O_{liq}$ = -14.98 ‰ (average δ^2H_{vap} = -186.3 ‰ and $\delta^{18}O_{vap}$ = -24.3 ‰ at average temperature of 23.8 °C); and KD with δ^2H_{liq} = -0.92 ‰ and $\delta^{18}O_{liq}$ = -0.01 ‰ (average δ^2H_{vap} = -80.4 ‰ and $\delta^{18}O_{vap}$ = -8.9 ‰ at average temperature of 22.9 °C).

Hydrogen and oxygen stable isotope values are reported in δ notation: $\delta = (R_{sample}/R_{standard} - 1)$, where R_{sample} and $R_{standard}$ are the $^2H/^1H$ or $^{18}O/^{16}O$ ratios for the sample and standards respectively, and values are reported in per mille (parts per thousand, ‰). Water vapor δ values are calibrated to the Vienna Standard Mean Ocean Water (VSMOW) scale (Coplen, 1994) by analyzing liquid water standards at the beginning and end of each sample set.

Aliquots of ~3 g of U_3O_8 powder were contained in open 20 mL glass vials placed inside each chamber. The U_3O_8 powder was distributed evenly across the bottom of each vial, forming a disc ~2 cm in diameter, with ~1 mm thickness, though this volume diminished throughout the exposure experiments as the powders were sampled. Two separate humidity exposure experiments were conducted: 1) exposure of U_3O_8 to KD-vapor for 90 days, and 2) remaining material from the 90-day KD vapor experiments were transferred to TWW-vapor chambers for another 90 days of TWW-vapor exposure.

2.3 SEM and TEM analytical methods

Aliquots of U_3O_8 from all humidity exposure levels were analyzed after the exposure experiments by scanning electron microscopy (SEM) to reveal the morphology and texture of the powders. Aliquots of material were dispersed on carbon adhesive tabs mounted on standard SEM pin stubs (Ø12.7mm x 8mm pin height), and SEM was performed with a JEOL JSM-7401F FE-SEM at an accelerating voltage of 5 kV.

Transmission electron microscopy (TEM) was performed after the exposure experiments on the material from the 91% RH exposure to reveal microstructural detail of the powders. TEM thin section specimens were prepared by focused ion beam (FIB) technique using a FEI Nova 600 dual beam microscope comprising a Ga+ liquid metal source FIB and a field emission gun SEM. A Pt strap was applied onto the top surface of a TEM slice by in-situ deposition induced firstly by electron beam (e-Pt coating) and then by ion beam (i-Pt coating) to protect the material

surface structure from bombardment damage during FIB cutting. TEM analysis was done using a FEI 80-300kV Titan transmission electron microscope operating at 300 kV.

2.4 TGA-IRIS analytical methods

To make δ^2H and $\delta^{18}O$ measurements of secondary mineralization hydration water, a TA Discovery thermogravimetric analyzer (TGA) (TA Instruments, New Castle, DE, USA) with infrared-heated furnace and 25 position sample changer was connected to a Picarro L-2130i cavity ring down isotope ratio infrared spectroscopy (IRIS) water isotope analyzer (Picarro Inc., Santa Clara, CA, USA) by a sample transfer line heated to 80 °C (Oerter et al., 2017). Water vapor generated by sample heating in the TGA is carried through the system by N_2 carrier gas, flowing at 30 mL min^{-1}.

Duplicate samples of U_3O_8 were taken from each humidity chamber at Day 0, 1, 2, 5, 8, 11, 15, 20, 29, 40, 50, 59, 70, 78, 90, and single samples at Day 91, 92, 94, 97, 100, 105, 111, 120, 146, 160, and 180. At each sampling event, aliquots of U_3O_8 (60 to 80 mg) were loaded into pre-tared aluminum sample holders and immediately hermetically crimp-sealed with lids to prevent exposure to ambient humidity (<5 min exposure time). All TGA-IRIS analyses began with the autosampler opening each sample holder lid, loading the sample into the TGA furnace, and immediately closing the furnace. The TGA furnace was held at 35 °C and purged with dry N_2 for 5 minutes to flush the system of any ambient water vapor and return $[H_2O]$ values in the IRIS instrument to ≤ 200 ppmV.

To first identify the U_3O_8 material's water release temperature ranges for subsequent isotope measurements, an initial aliquot was heated at a constant rate of 10 °C min^{-1} from 35 to 500 °C ("ramp heated"). Based on the ramp heating results (discussed more below), samples for hydrogen and oxygen stable isotope analysis were heated at a very fast rate of ≥ 25 °C sec^{-1} ("step heated") to rapidly release all of the water available in each temperature range as a single pulse of sufficient peak size for reliable IRIS oxygen and hydrogen stable isotope analysis. The isothermal dwell time at each heating step was 10 minutes for complete dehydration at each temperature. The same samples were then step heated to 350 °C to release mineral hydration water, again followed by 10 min isothermal dwell time.

2.4 Fluorination and IRMS analytical methods

To make measurements of the total oxygen isotope composition in a sample (structural oxygen in U_3O_8 and $UO_3{\bullet}2H_2O$, and hydration water in $UO_3{\bullet}2H_2O$), which we denote as $\delta^{18}O_{Total}$, we analyzed samples of U_3O_8 with varying amounts of metaschoepite ($UO_3{\bullet}2H_2O$) present (specific samples described more below) by fluorination and isotope ratio mass spectrometry (IRMS). Samples of 30 to 40 mg where placed into nickel crucibles inside nickel reaction vessels and pre-fluorinated with 140 torr ClF_3 at ~25 °C for 5 minutes. This pre-fluorination step was conducted to remove any adsorbed water vapor on the sample or any reaction products inside the nickel vessels resulting from sample loading. The pre-fluorination products are pumped away and 590 torr ClF_3 was loaded into each nickel reaction vessel and heated at 550 °C for 4 hours. Liberated O_2 was passed through two LN_2 traps to remove any condensable gases and a heated NaCl trap to remove F_2, and then collected on 13X molecular sieve at LN_2 temperature. The 13X sieve was then warmed to room temperature, and the O_2 was transferred to an IsoPrime-100 spectrometer operating in dual-inlet mode. No standard reference materials are currently available for oxygen

isotope compositions in U_3O_8. Values of $\delta^{18}O_{Total}$ were calibrated relative to VSMOW based on analysis of the silica sand standard NBS-28 (quartz, $\delta^{18}O_{Total}$ = 9.6‰) which were analyzed in duplicate during each fluorination run. Precision for $\delta^{18}O_{Total}$ values determined on standard deviation of the calibration standards was ±0.11‰.

3. Results

3.1 Thermal water release profiles

To assess the H_2O release profiles during TGA heating for uranium oxide samples, and to determine the appropriate step-heating scheme for subsequent water vapor isotope analysis, we heated an aliquot of the U_3O_8 starting material in the TGA (without isotope analysis) from 35 to 500 °C at a constant rate (ramp heating) of 10 °C min^{-1}. Ramp heating at 10 °C min^{-1} of this material resulted in a two-step mass loss profile, with initial mass loss occurring from ~50 to ~105 °C, followed by another interval from ~250 to 350 °C (Fig. 1). After the humidity exposures, the samples had similar mass release profiles. Based on these mass loss profiles with ramp heating, we determined the heating scheme to release the water available at each temperature step in a single pulse for isotope analyses to be step-heating first to 105 °C followed by 10 minutes isothermal at 105 °C, and then step-heating to 350 °C followed by 10 minutes isothermal at 350 °C.

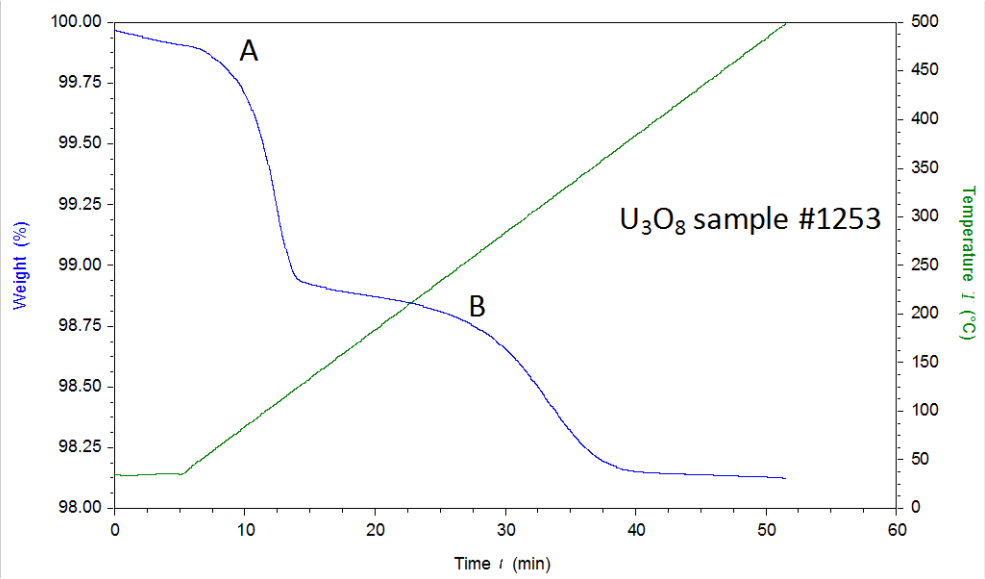

Figure 1. Mass loss (% relative to starting sample mass) for a sample of the starting U_3O_8 material (blue line) with constant heating from 35 to 500 °C at 10 °C min^{-1} (green line); (A) represents mass loss from ~50 to 105°C, and (B) represents mass loss from ~250 to 350 °C.

3.2 Water accumulation with humidity exposure

The accumulation of water on the sample particle surfaces from exposure to humid air can be measured as an increase in mass loss during TGA heating. Mineral hydration rates were determined as water mass accumulation rates calculated from linear regressions of the data arrays of mass loss upon heating shown in Figure 2, assuming all mass difference from the start of the exposure experiments was accumulated water. Water accumulation rates for the water yielded at 105 °C and 350 °C are shown in Table 1. U_3O_8 in our experiments only accumulated water at 91% RH (Fig. 2). The rates of water mass accumulation for U_3O_8 available at 350 °C are approx. 50% to 60% of that available at 105 °C (Table 1).

Table 1. Water mass accumulation rates for U_3O_8 samples in the humidity exposure experiments expressed as % mass loss day^{-1} upon heating in TGA-IRIS analysis. Only those with non-zero water accumulation rates are shown.

Material	Experiment	RH	% loss day^{-1} @ 105 °C	R^2	% loss day^{-1} @ 350 °C	R^2
U_3O_8	KD 90 day	91%	0.0028	0.95	0.0015	0.77
U_3O_8	KD -> TWW 180 day	91%	0.0026	0.94	0.0016	0.90

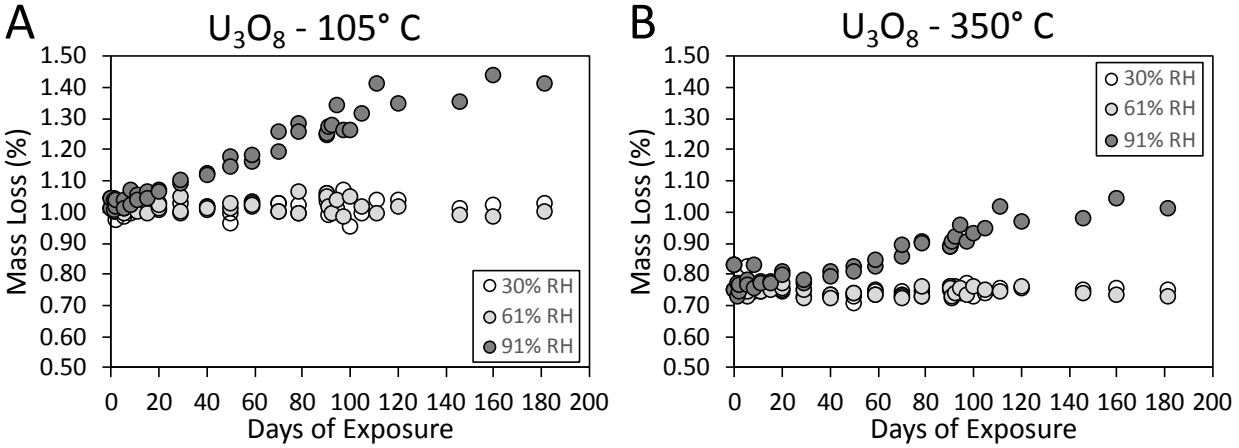

Figure 2. Plots of the mass loss upon heating in the TGA-IRIS to (A) 105 °C and (B) 350 °C for U_3O_8 exposed to KD water vapor for 90days, and then TWW water for another 90 days.

3.3 Secondary mineralization from humidity exposure

Analysis by XRD of the U_3O_8 material before humidity exposure show that the starting material was dominated by α-U_3O_8, with minor metaschoepite ($UO_3 \cdot 2H_2O$) present. This minor pre-existing secondary mineralization is likely from intermittent ambient humidity exposure since material synthesis in the 1980's. After 90 days of exposure, the samples of U_3O_8 from all of the humidity levels were re-examined by XRD and all had measurable metaschoepite present.

After the second 90 day exposure (180 days total) all samples had metaschoepite still present. There was no evidence of transformation of metaschoepite to schoepite.

A comparison of the SEM analyses of the samples exposed to 30%, 61%, and 91% RH for 180 days shows that platy-tabular crystals of secondary mineralization occur on the surfaces of the U_3O_8 particles (Fig. 3). Due to the lack of crystal structural information from the SEM observations, we are not able to unambiguously determine from the SEM observations that these crystals are strictly the result of secondary mineralization from humidity exposure. In addition, the U_3O_8 material itself has some layered structural morphology, further increasing the difficulty in resolving the secondary mineralization by SEM imaging. However, the abundance and size of these tabular mineral crystals does correlate with increased exposure humidity (Fig. 3).

To further determine the nature of the secondary mineralization formed during humidity exposure, we examined a sample of starting material (unexposed U_3O_8) and the U_3O_8 sample exposed to 91% RH for 180 days total (first KD-water vapor for 90 days then TWW-water vapor for another 90 days) by using TEM imaging and electron diffraction analysis. Tabular shaped secondary mineral phases are identified from both samples in addition to the primary micrometer-sized U_3O_8 crystals (Fig. 4A and 4F). In the sample of starting material (unexposed U_3O_8), the secondary phase predominantly formed on the surfaces of U_3O_8 particles and occasionally bridged U_3O_8 particles (Figs. 4A-4C). Characteristic selected-area electron diffraction patterns taken from the larger, micrometer-sized particles match that of single α-U_3O_8 crystals with good crystallinity (Figs. 4D and 4I). In the humidity-exposed sample, more abundant additional secondary phases grew between the U_3O_8 particles, displaying distinctive tabular shapes that are sub-micrometer in thickness (Figs. 4F-4H). Bright-field (Fig. 4G) and dark-field (Fig. 4H) TEM images show a tabular secondary mineralization crystal that grew between U_3O_8 particles. Growth of these tabular secondary mineral phases are a signature of uranium oxide that has been subjected to high-humidity exposure (Donald et al., 2017).

The electron diffraction pattern taken from the secondary phase formed on the surface of the starting material (unexposed U_3O_8) displays a polycrystalline ring-pattern overlapping a diffuse scattering of an amorphous matrix (Fig. 4E), of which the polycrystalline ring-pattern matches that of UO_2, inferring alteration products of schoepite or metaschoepite. In the case of the humidity-exposed U_3O_8 sample, an electron diffraction pattern from a sub-micrometer sized tabular secondary mineralization phase displays a more predominant ring pattern diffraction feature in which the primary reflection rings match polycrystalline UO_2 (Fig. 4J). Importantly, extra reflections matching that of metaschoepite are also present near to the central transmitted spot (inset of Fig. 4J). These extra reflections have d-spacings of 0.73, 0.52, 0.40 and 0.36 nm, corresponding to increasing distance from the central transmitted spot, which can be attributed to a mixture of schoepite/metaschoepite (Finch et al., 1996; Finch et al., 1997; Finch et al., 1998) and dehydrated schoepite, likely as γ-uranyl dihydroxide (Siegel et al., 1972).

We also analyzed by XRD a sample of the U_3O_8 that had been exposed to KD-water vapor at 91% RH for 90 days, both before and after TGA-IRIS heating and analysis at 350 °C. Before heating, the U_3O_8 sample that had been exposed to 91% RH for 90 days had a metaschoepite component along with the primary α-U_3O_8 (Fig. 5). After heating to 350 °C for TGA-IRIS analysis, the metaschoepite was eliminated but the α-U_3O_8 remained and displayed no crystal structure transformation (Fig. 5).

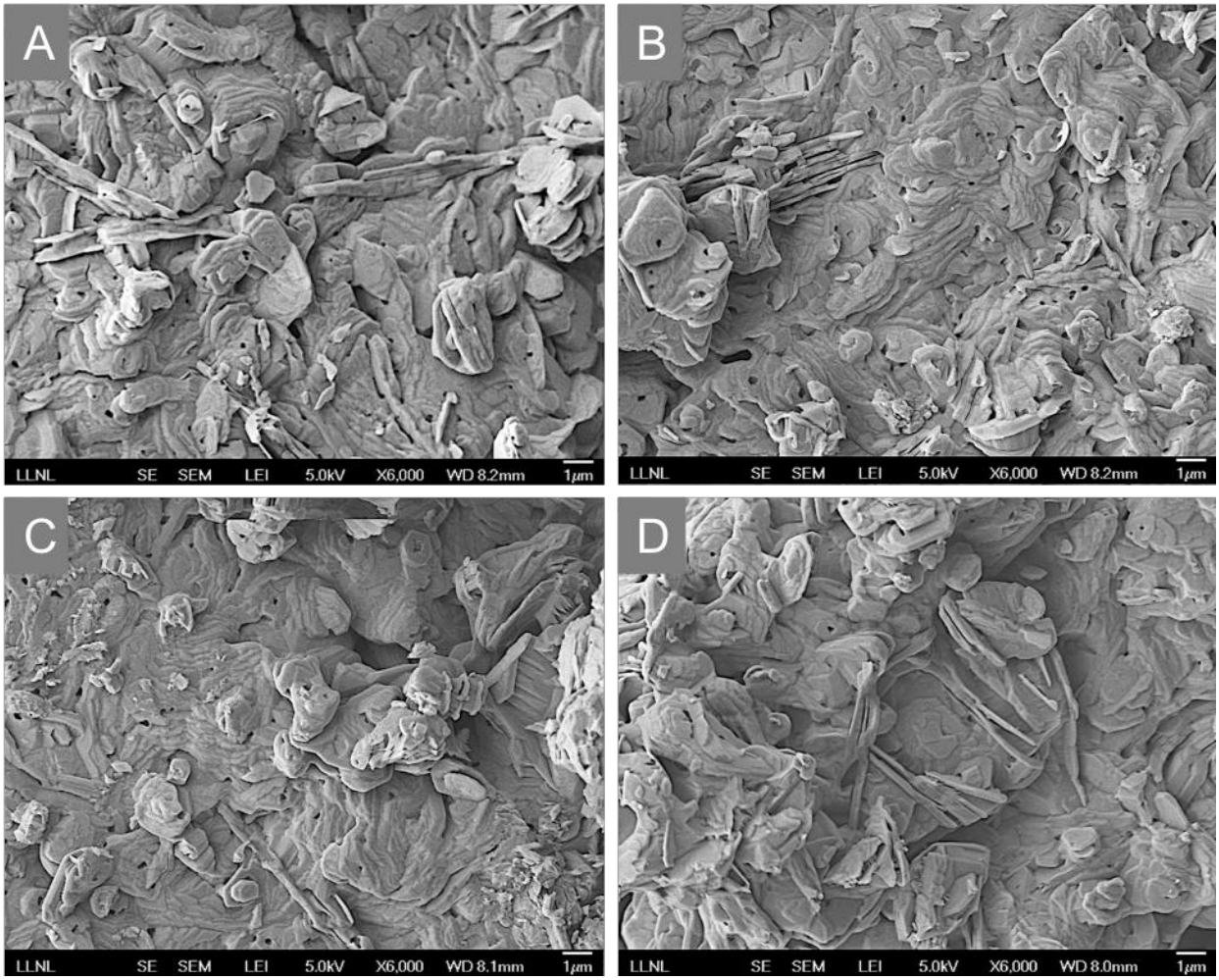

Figure 3. Secondary electron SEM images showing typical morphology of U_3O_8 powders: (A) starting material, and material exposed to (B) 30%, (C) 61%, and (D) 91% RH KD-water vapor for 90 days, then switched to TWW-water vapor for another 90 days (180 days total humidity exposure).

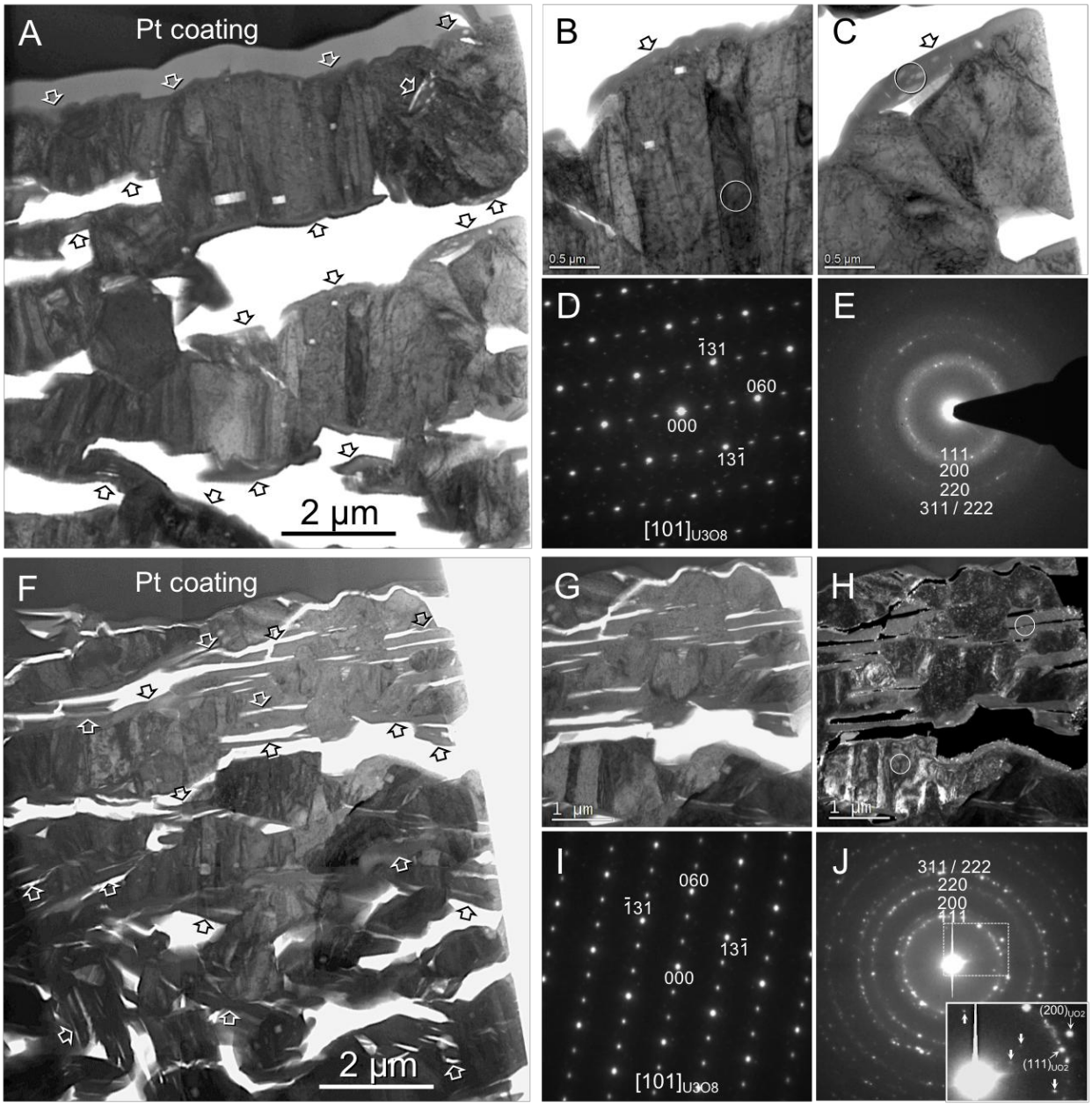

Figure 4. TEM observation and electron diffraction analysis of the sample before exposure (A-E) and the sample exposed to 91% RH for 180 days (F-J). (A) and (F) are bright-field TEM images of FIB sections where arrowheads indicate the alteration products of mateschoepite or schoepite formed either on the surface of or between U_3O_8 particles. (B) and (C) are bright-field TEM images of a closer looking of the alteration product of metschoepite formed on the surface of U_3O_8. (D) and (E) are selected-area electron diffraction patterns collected from U_3O_8 (circled in white on (B)) and alteration products of schoepite (circled in white on (C)). Bright-field (G) and dark-field (H) TEM images show a closer looking of tabular schoepite/metaschoepite crystal that grew between U_3O_8 particles. (I) and (J) are selected-area electron diffraction patterns collected from the U_3O_8 (circled in white at lower-left corner on (H)) and the tabular product (circled in white at upper-right corner on (H)). The ring patterns (E) and (J) are indexed

matching crystal structure of UO_2. Besides the reflection rings of UO_2, some extra reflections can be identified in (J), as indicated by the thicker arrowheads on the inset which is an enlarged pattern of the part enclosed in the white dash-line box.

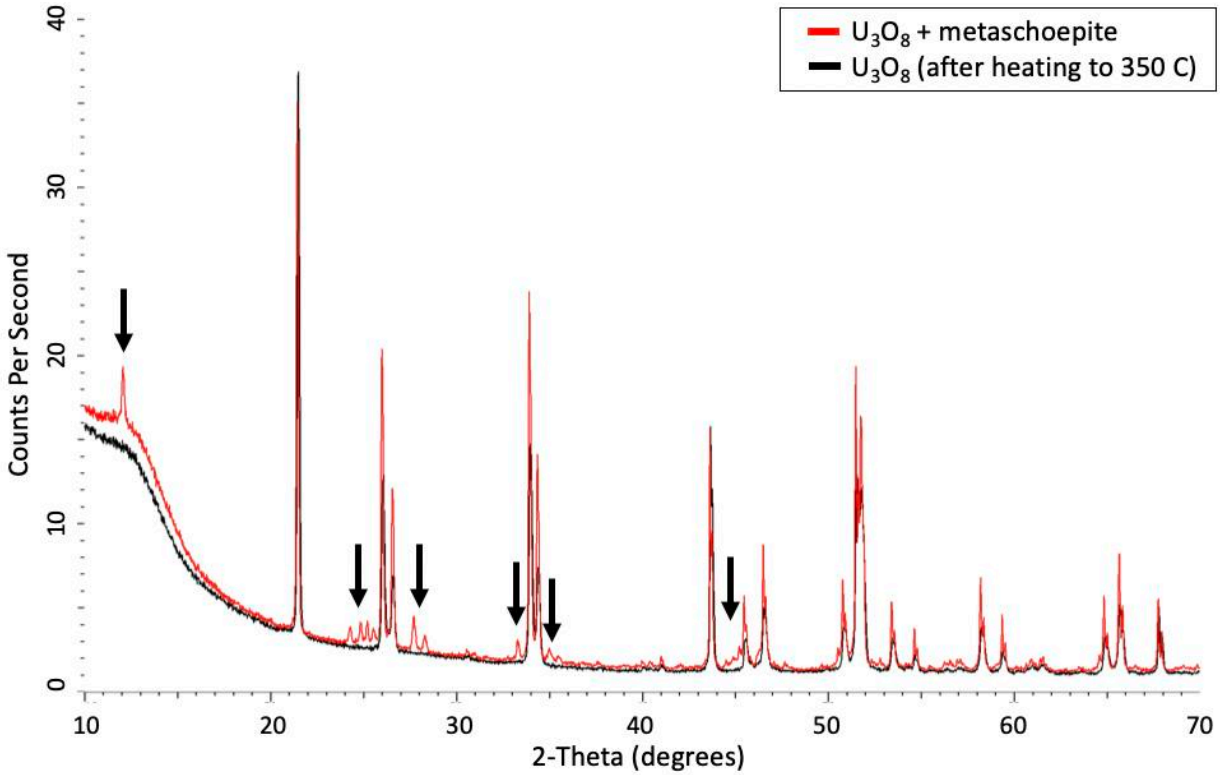

Figure 5. Phase analysis by XRD from pre- and post-heating of 91% RH-exposed U_3O_8 to 350°C during TGA-IRIS analysis. Red line shows XRD diffraction pattern of U_3O_8 material before heating, black arrows indicate diagnostic metaschoepite reflections, and black line shows XRD diffraction pattern of the same sample post-350 °C heating without metaschoepite and no transformation of U_3O_8 crystal structure.

3.4 Stable isotope measurements by TGA-IRIS

3.4.1 Precision of isotopic measurements

We estimate the internal precision, or the variability between replicate measurements of the same material, by calculating the standard deviation of the TGA-IRIS isotope measurements of the two replicate samples of each material taken during each sampling event, and these results are shown in Table 2. This approach captures the variability between TGA-IRIS measurements made on each material that was exposed to differing humidity levels, with differing exposure duration, as well as the variability in measurements made on water yielded at 105 °C and 350 °C.

For U_3O_8 measurements made at 105 °C the internal precision for δ^2H ranged from 3.33‰ to 6.01‰, and for $\delta^{18}O$ was 0.69‰ to 0.84‰ (Table 2). For measurements made at 350 °C δ^2H values ranged from 3.55‰ to 5.86‰, and for $\delta^{18}O$ was 0.20‰ to 0.33‰. No clear trends

in the internal precision figures with humidity levels are present for U_3O_8. No standard reference materials for the isotopic composition of mineral hydration waters are available. However, the external precision on goethite synthesized with water of known isotopic composition using the same instrument and analytical approach used here were reported as 0.3‰ to 1.6‰ for δ^2H, and 0.17‰ to 0.27‰ for $\delta^{18}O$ (Oerter et al., 2017). Based on these various metrics, we take the most conservative values and estimate the overall precision of TGA-IRIS measurements made on metaschoepite on U_3O_8 at 105 °C as 6.01‰ for δ^2H values, 0.84‰ for $\delta^{18}O$ values, and at 350 °C as 5.92‰ for δ^2H, and 0.33 for $\delta^{18}O$.

Table 2. Estimated internal precision of TGA-IRIS isotope measurements of metaschoepite, calculated as the average of standard deviations calculated from pairs of measurements through the first 90 day humidity exposures.

			105 °C		350 °C	
Material	Experiment	RH	δ^2H St. Dev. ‰	$\delta^{18}O$ St. Dev. ‰	δ^2H St. Dev. ‰	$\delta^{18}O$ St. Dev. ‰
U_3O_8	KD 90 day	30%	3.33	0.69	3.55	0.33
U_3O_8	KD 90 day	61%	6.01	0.84	5.92	0.23
U_3O_8	KD 90 day	91%	5.80	0.81	5.86	0.20

3.4.2 Stable isotopic composition of metaschoepite hydration water

The δ^2H and $\delta^{18}O$ values of water recovered from U_3O_8 exposed to KD-vapor for 90 days are shown in Figure 6. Water yielded by TGA heating at 105 °C and 350 °C have δ^2H values that exhibited broadly similar trends, though with different δ^2H values, through the humidity exposures: 1) relatively low δ^2H values before the material was placed in the humidity chambers (Day 0), 2) then an increase of approximately 50‰ to maxima near Day 20, 3) followed by a slight decrease through the end of the exposures (Figs. 6A and 6B). There was not a clear influence of the δ^2H composition of the exposure water vapor on the δ^2H values of the metaschoepite hydration water. There were also no clear systematic differences in δ^2H values of metaschoepite hydration water between the various humidity exposures, except that δ^2H values from the 91% RH exposures tended to be higher than for 61% or 30% RH.

When the exposure water vapor for U_3O_8 was switched from high δ^2H values (KD-vapor) to lower δ values (TWW-vapor), the δ^2H values of the water metaschoepite hydration water yielded at both 105 °C and 350 °C showed distinct step-like decreases towards the isotopic values of the new exposure water vapor (Figs. 6A and 6B). The step decreases were of a similar magnitude in δ^2H values for both 105 °C and 350 °C but were not as large as the decrease in water vapor δ^2H values and did not match that of the new water vapor.

For $\delta^{18}O$ values of metaschoepite hydration water yielded at 105 °C from U_3O_8 exposed first to KD-vapor for 90 days, a similar pattern to the δ^2H values of the same material was found: low at the start, higher near Day 20, and a slow decrease through the end of the exposure, with no clear correspondence with $\delta^{18}O$ values of the exposure water vapor (Fig. 6C). In contrast, $\delta^{18}O$ values of metaschoepite hydration water yielded at 350 °C exhibited a distinct trend through the exposure: $\delta^{18}O$ values of the starting material (Day 0) were ca. -13‰ and metaschoepite hydration water yielded by TGA heating of material from all humidity exposures

showed increasing $\delta^{18}O$ values up to Day 15 (Fig. 6D), after which the isotopic values either levelled out and showed clear correspondence with the water vapor, in the case of 91% RH, or had isotopic values slightly lower than the water vapor for the 61% and 30% RH exposed samples. The 350 °C $\delta^{18}O$ values also had lower variability between replicates measured on the same day, compared to either 105°C $\delta^{18}O$ values or any $\delta^{2}H$ values.

When the exposure water vapor for the U_3O_8 was switched from high $\delta^{18}O$ values (KD-vapor) to lower δ values (TWW-vapor), the $\delta^{18}O$ values of the metaschoepite hydration water yielded at 105 °C showed a distinct step-like decrease towards the isotopic values of the new exposure water vapor but still did not match that of the new water vapor (Fig. 6C). For metaschoepite hydration water yielded at 350 °C $\delta^{18}O$ values showed a slight decrease but did not approach that of the new water vapor for the rest of the 90 day exposure (Fig. 6D). There was a systematic difference between different exposure humidities, with $\delta^{18}O$ values of water from the 91% RH humidity showing less shift after the vapor change and remaining at higher $\delta^{18}O$ values than water from the 61% or 30% exposure humidities.

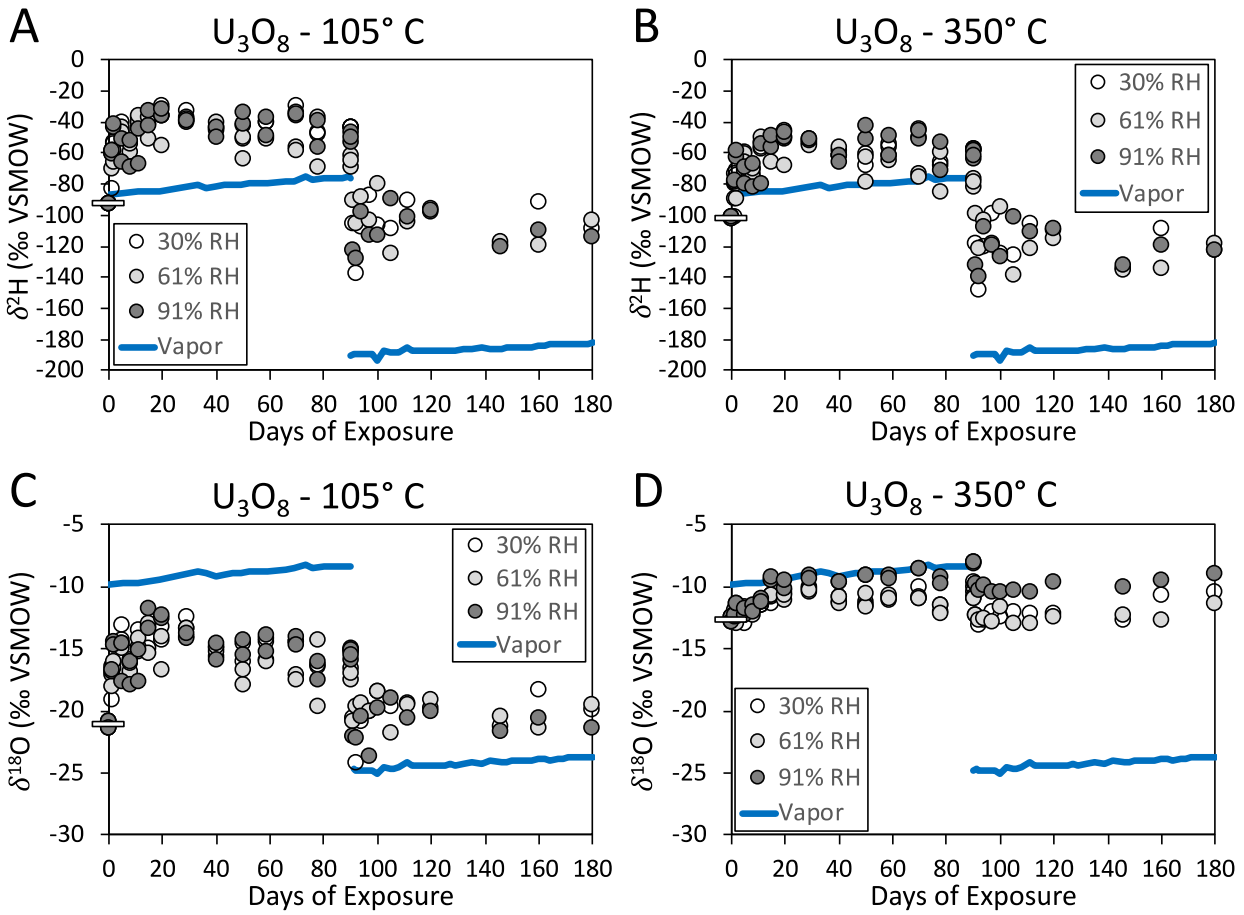

Figure 6. Isotopic results of metaschoepite hydration water formed on U_3O_8 exposed to KD-vapor for 90 days, and then exposed to TWW-vapor for an additional 90 days. Values of δ^2H and δ^{18}O of water from samples of U_3O_8 heated to 105 °C (A, C) and 350 °C (B, D) analyzed by TGA-IRIS. Starting material average δ^2H and δ^{18}O values are shown as white bars at Day 0. Water vapor data shown is from 61% RH exposure chamber. Precision of isotopic values are shown in Table 2.

3.5 O isotopic composition by fluorination and IRMS

To evaluate the O isotope effects of TGA heating on the underlying U_3O_8 and coexisting metaschoepite, we analyzed the δ^{18}O values of all of the oxygen (interlayer water and uranyl-bound, $\delta^{18}O_{Total}$) in the unexposed U_3O_8 starting material (Day 0) and of U_3O_8 samples exposed to KD-vapor for 90 days, followed by exposure to TWW-vapor for another 90 days (Day 180), by fluorination and IRMS. Importantly, $\delta^{18}O_{Total}$ does not include any water adsorbed to particle surfaces because the samples were pre-flourinated to remove any water in the fluorination system. Aliquots of each sample type were analyzed before and after heating to 350 °C during TGA-IRIS analysis (n=2 replicates for each sample type). The results are shown in Table 3.

The samples that represent the unexposed U_3O_8 starting material (Day 0) had average $\delta^{18}O_{Total}$ values of 12.0‰, and there was not a difference (within analytical precision) between

the unheated material samples, and those that had been heated to 350 °C. For the samples that had been exposed to 91% RH for 180 days, the average $\delta^{18}O_{Total}$ value of the unheated samples was 10.89‰, and was 9.85‰ for samples that had been heated to 350 °C (Table 3).

Table 3. Values of $\delta^{18}O_{Total}$ from fluorination and IRMS analyses.

		Unheated	After TGA-IRIS heating to 350 °C
Sample	Replicate	$\delta^{18}O_{Total}$ ‰	$\delta^{18}O_{Total}$ ‰
U_3O_8, Starting Material	1	12.06	11.96
U_3O_8, Starting Material	2	11.98	12.13
	Average	12.02	12.04
U_3O_8, KD -> TWW, Day 180	1	10.95	9.98
U_3O_8, KD -> TWW, Day 180	2	10.83	9.73
	Average	10.89	9.85

4. Discussion

4.1 Secondary mineralization of U_3O_8 under humidity exposure

The secondary phases observed by TEM and electron diffraction formed on and between the primary U_3O_8 particles are secondary mineralization products composed of metaschoepite. These products were formed by U_3O_8 reacting with H_2O through sorption, oxidation, dissolution and precipitation processes under an oxidizing environment in the humidity exposure experiments.

During TGA-IRIS analysis, mass lost in the 50 to 105 °C interval represents dehydration of weakly-adsorbed water on mineral surfaces (Foldvari, 2011; Oerter et al., 2017). Although there is no increase in mass loss, and thus a lack of surface-sorbed water accumulation at 30% and 61% RH, compared to the linear increase in surface-sorbed water with exposure time for the samples exposed to 91% RH (Fig. 2A), the isotope values of these desorbed waters show a similar pattern (Figs. 6A and 6C). These similar isotope values suggest that this water originates from the same source, or combination of sources.

Under a low or middle humidity, it will take a much longer time to form metaschoepite because of a limitation in the amount of H_2O adsorbed on the surface of U_3O_8 and slow dissolution rate of the U_3O_8. The case observed for the starting material belongs to this case, in which the minor metaschoepite on the surface of the starting material U_3O_8 formed during a long period of material storage. The inference in the case of the unexposed U_3O_8 starting material is case is that the U_3O_8 particles have not been subjected to a high humidity environment.

The increase in the amount of surface-sorbed water for the 91% RH samples (Fig. 2) suggests that this extra water is stored on the particle surfaces in a different form than for the lower humidity samples. Indeed, humidity levels of ~30% correspond to 1 monolayer of water

adsorbed to particles surfaces, ~60% to 2 monolayers, and ~90% to 5 monolayers. This variable amount of water present at the particle surfaces may lead to the formation of surface hydroxyls to different degrees and at different rates, as has been shown for various uranium oxide minerals (Finch et al., 1992). At the 91% RH level, there are likely to be localized aqueous-saturated environments present on the particle surfaces, which result in the nucleation and growth of hydrated uranium minerals (Finch et al., 1992; Donald et al., 2017). In the case observed for the sample exposed to 91% RH for 180 days, the hydrated phase was metaschoepite, which formed by reacting with H_2O supplied as vapor in the exposure chambers. These various surface hydration and mineral precipitation mechanisms, along with the water accumulation trends shown in Fig. 2 suggest that there is a humidity threshold between 61% and 91% RH that leads to increased surface water accumulation and hydrated mineral formation on U_3O_8 particles.

Analyzing a sample by XRD that had been exposed to 91% RH both before and after heating to 350 °C allowed the mineralogical source of the water yielded at that temperature during TGA-IRIS analysis to be determined. Before heating, the sample had a distinct metaschoepite component along with α-U_3O_8 (Fig. 5). After heating to 350 °C, the metaschoepite was eliminated but the α-U_3O_8 remained and was not affected by the heating (Fig. 4). Thus, mass lost during heating in the 250 to 350 °C interval (Fig 1) is water held within the metaschoepite crystal structure in the interlayers between sheets of uranyl ions.

In the case of the UO_2 crystallites associated with the metaschoepite in the starting material (Fig. 4E), these may have formed by phase transformation from the metaschoepite during material storage due to possible variations of humidity and temperature. In the 180-day exposure at 91% RH sample the UO_2 crystallites associated with the secondary tabular metaschoepite phases (Fig. 4J) may have formed by phase transformation from the metaschoepite that was induced under focused ion beam bombardment during TEM sample preparation. The metaschoepite is also sensitive to electron beam illumination. We are, therefore, unable to exclude that some of the UO_2 crystallites could be an artefact of sample preparation or by electron beam illumination during TEM analysis. Although the initial crystal structure of metaschoepite is unable to be completely retained in TEM analysis, its morphology is retained and distinguishable from that of the primary U_3O_8 phase in TEM imaging, and it is therefore useful for investigation of the secondary mineralization.

4.2 Evaluation of isotope exchange between mineral water reservoirs

A central question in the use of TGA-IRIS to analyze hydrogen and oxygen stable isotope signatures of hydration water in uranium oxide materials is: To what degree do the uranium oxides phases undergo chemical and physical changes during TGA-IRIS analysis, and do these physicochemical changes result in hydrogen and/or oxygen isotope exchange? The lack of crystal structure alteration of the U_3O_8 after heating indicates that neither the surface-sorbed water yielded upon heating at 105 °C, nor the metaschoepite structural water yielded at 350 °C interacts with or alters the U_3O_8 crystal structure of the material itself during TGA-IRIS analysis.

In terms of the stable isotope composition of metaschoepite hydration water, the simultaneous presence of more than one “reservoir” of hydrogen and oxygen on and in the U_3O_8-metaschoepite mineral complexes, indicates that it is important to evaluate the degree to which each element can move between each reservoir. If exchange can occur between each reservoir, and if the reservoirs have different isotopic compositions, with respect to each element, then the measured isotopic composition will not be indicative of the source of the water within the mineral.

In metaschoepite hydrogen exists as water adsorbed to particle surfaces and as interlayer water between the uranyl sheets (Plasil, 2018). Oxygen in metaschoepite exists in these reservoirs, but also as oxygen bonded to uranium in the uranyl sheets. Isotopic exchange could occur between these reservoirs for each element during or after mineral formation, as well as during heating at 105 °C and then 350 °C for TGA-IRIS analysis. A simple test for isotope exchange is comparison between values of the water vapor yielded at each temperature, provided that the isotopic composition is different in each reservoir. If exchange has occurred there will be a correlation between δ values of the water vapor yielded at each temperature step.

For hydrogen, there are strong correlations between δ^2H values yielded at 105 °C and at 350 °C that ranges from $R^2 = 0.94$ to 0.99, with slopes from 0.92 to 1.05, and intercepts from -20.5 to -10.0 (Fig. 7A). The tight correlations and slopes that are parallel to each other and the 1:1 relationship between the two temperatures indicate that there is hydrogen isotope exchange between water adsorbed on particle surfaces and that held in interlayers during heating for TGA-IRIS analysis. However, it appears from linear data arrays that are offset from 1:1 that there is a difference in the isotopic composition of each water reservoir within the mineral, and that there is not exchange during or after mineral formation. The fractionation factor for adsorbed water appears to be 10‰ to 20‰ higher than that of the water held in interlayer spaces (Fig. 7A). Mixing of the two reservoirs during TGA-IRIS heating does not explain the apparent fractionation because the amount of water in the reservoirs would have to be the same to result in such consistent offsets from 1:1, and the water yields increase through time for the 91% RH exposures (Fig. 2).

For oxygen, there are not correlations between $\delta^{18}O$ values yielded at 105 °C and at 350 °C, with $R^2 = 0.33$ to 0.58 (Fig. 7B), indicating that there is not oxygen isotope exchange between water adsorbed on particle surfaces and that held in interlayers during heating for TGA-IRIS analysis. However, the data arrays of the KD-vapor exposed samples do plot about 6‰ above the 1:1 line in Figure 7B, though with considerable scatter, indicating that the oxygen fractionation factor of the interlayer water is about 6‰ higher than that of the adsorbed water. The samples that were switched into the TWW-vapor after KD-vapor exposure have a larger deviation from the 1:1 line, but this is probably due to the adsorbed water (105 °C) showing more response to the change to TWW-vapor with low $\delta^{18}O$ values (discussed more below).

4.3 O_{Total} isotopic composition by fluorination and IRMS

The total O isotope composition (structural oxygen in U_3O_8 and $UO_3 \bullet 2H_2O$, and hydration water in $UO_3 \bullet 2H_2O$), of the Day 0 samples, was 12.0‰ and was the same for unheated Day 0 samples, and those that had been heated to 350 °C. This similarity in $\delta^{18}O_{Total}$ values indicates that: (A) heating to 350 °C does not have an effect on the O isotope composition of the underlying U_3O_8 material, and (B) that the pre-existing metaschoepite on the starting material was of such small quantity that its O_{Total} isotopic composition did not have a measurable influence on that of the whole sample U_3O_8 $\delta^{18}O_{Total}$ value.

For the samples that had been exposed to water vapor at 91% RH and had newly-formed metaschoepite on the particle surfaces, the average $\delta^{18}O_{Total}$ value was 10.89‰, which is 1.13‰ lower than the Day 0 samples. The lower $\delta^{18}O_{Total}$ value of the Day 180 samples probably results from the inclusion of water from the exposure humidity with lower $\delta^{18}O$ values into the hydration water of the metaschoepite ($UO_3 \bullet 2H_2O$). There could also be oxygen with lower $\delta^{18}O$ values from the water vapor included into the structural oxygen of the UO_3 group in the metaschoepite, which was re-incorporated into the U_3O_8 of the Day 180 samples after

dehydration at 350 °C. This water vapor-derived oxygen in the heated Day 180 samples leads to an average $\delta^{18}O_{Total}$ value of 9.85‰, which is 1.04‰ lower than that of the non-heated Day 180 samples, and 2.19‰ lower than the Day 0 samples. This incorporation of water vapor-derived oxygen into the residual U_3O_8 material from the 91% RH-exposed samples, but not the Day 0 samples may be a matter of there not being enough water available in the minor pre-existing metaschoepite on the Day 0 samples to contribute enough oxygen to be detectable. Indeed, the 91% RH exposed samples do not begin to accumulate significant metaschoepite hydration water until about Day 20 of the humidity exposures (Figure 2B).

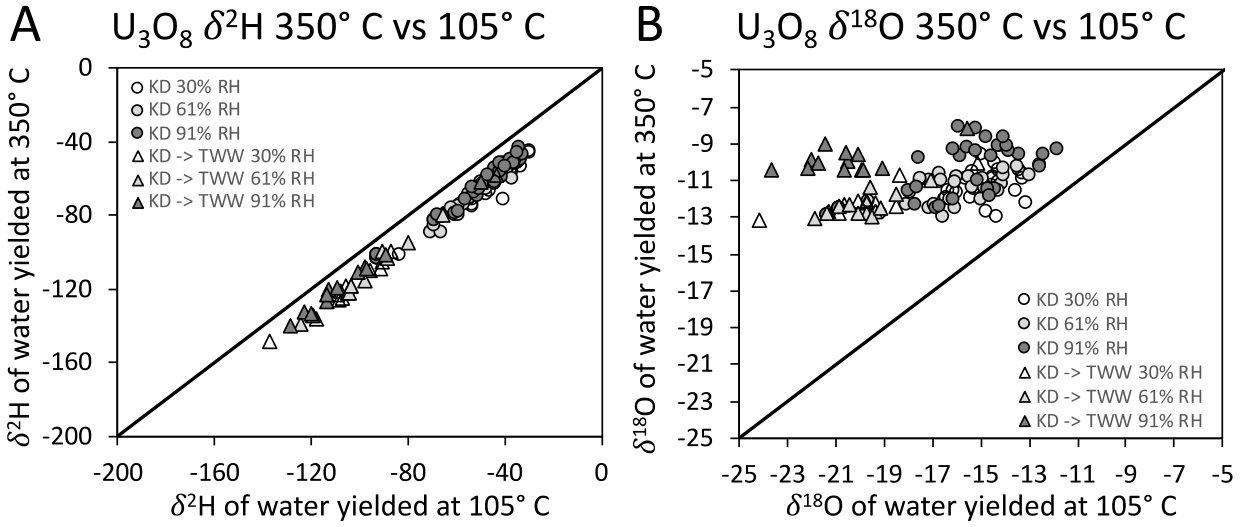

Figure 7. Comparison of δ values of water released from U_3O_8 at 105 °C and 350 °C for (A) δ^2H and (B) $\delta^{18}O$ from 90 day water vapor exposure experiments with KD-vapor ("KD"), and 180 day isotope reversal experiment from KD- to TWW-vapor ("KD → TWW"). Solid line is 1:1.

4.4 Hydration water isotopic composition and its durability

The exchangeability of hydrogen between adsorbed and interlayer water, and the lack thereof for oxygen helps explain some of the patterns observed in the δ values of the humidity exposure experiments. In this discussion, we assume that the water released at 105 °C represents the adsorbed water and that the interlayer water is released at 350 °C. The initial rise towards higher δ^2H values for the first 20 days in all of the humidity exposures (Fig. 6C) could be explained by mixing of the adsorbed water with some water with higher δ^2H values (and then exchange with the interlayer water during TGA-IRIS analysis). However, there is not a water source identified in this study with such a high δ^2H value. Some insight is gained from the gradual return to the KD-vapor in the exposures from 20 to 90 days, as was expected. We suggest that this early rise-gradual return pattern could be explained by a kinetic isotope fractionation effect happening at the particle surfaces. If the surfaces are not water saturated, as would be expected at the beginning of the humidity exposures, there could be a kinetic isotopic fractionation similar to evaporation taking place as water at the particle surface is not in

equilibrium with the surrounding vapor. This effect would diminish through time as the two water reservoirs come into equilibrium and the effect is minimized.

When the switch to TWW-vapor occurred at 90 days, there was a distinct step towards lower δ^2H values of both adsorbed and interlayer water, though not to the full extent of the change in exposure vapor (Figs. 7C and 7D). The lesser shift could be explained by preexisting water not fully being replaced by the new vapor. In the case of hydrogen, the remarkably similar patterns through time of the adsorbed (105 °C) and interlayer (350 °C) water δ^2H values are explained by the exchangeability of hydrogen during TGA-IRIS heating.

For oxygen, the pattern in the adsorbed $\delta^{18}O$ values is very similar to that of δ^2H, suggesting similar processes are occurring, which supports the kinetic fractionation effect due to the disequilibrium between adsorbed water and exposure vapor scenario discussed above. After the switch from KD-vapor to TWW-vapor at 90 days, the adsorbed water $\delta^{18}O$ values almost approach that of the new exposure vapor, but don't ever fully match, supporting the incomplete replacement of preexisting adsorbed water.

The $\delta^{18}O$ values of interlayer (350 °C) water display the most organized response to exposure humidity and attain isotopic equilibrium with the exposure humidity in about 15 days for 91% RH, which is maintained for the rest of the KD-vapor exposure (Fig. 6B). The lower humidity exposures show a similar shift towards the exposure vapor $\delta^{18}O$ values within 20-25 days, but never fully match, and may move to slightly lower $\delta^{18}O$ values through the 90 day exposures, though variability in the data make it hard to resolve a distinct shift (Fig. 6B). After the switch to TWW-vapor with lower δ values at 90 days, the interlayer water $\delta^{18}O$ values show a subtle shift lower, but of only a few ‰ and maintain these new values throughout the remainder of the exposures. The difference between the $\delta^{18}O$ values from the 91% RH exposures, and that of the 61% and 30% RH exposures (which are essentially the same), suggests that there is a humidity threshold between 61% and 91% in the response of the oxygen stable isotope composition of the interlayer water in metaschoepite to the relative humidity it forms in. Below 61% the oxygen stable isotope composition of metaschoepite does not fully attain that of the exposure atmosphere, but at 91% RH it does, suggesting that higher humidity is required to form new metaschoepite. The constant $\delta^{18}O$ values of interlayer water in metaschoepite throughout the humidity exposures regardless of humidity level suggest that once formed, metaschoepite $\delta^{18}O$ values are stable and durable, even if the oxygen isotope composition of the exposure humidity changes.

5. Conclusions

We determined that when U_3O_8 is exposed to humid air, metaschoepite secondary mineralization will form on the surface of the U_3O_8 particles at high humidity levels. The hydrogen and oxygen stable isotope composition of the water adsorbed to the particle surfaces and that incorporated into the mineral as hydration water is measurable by TGA-IRIS without affecting the underlying U_3O_8 material. Hydrogen in the various water reservoirs is highly exchangeable and thus the δ^2H data of these waters is not easily interpreted. However, oxygen in the separate water reservoirs is much less exchangeable, and thus $\delta^{18}O$ values of the metaschoepite interlayer water is likely to reflect that of the water the sample was exposed to. The oxygen isotope signature of the interlayer water in metaschoepite also appears to be fairly durable, and once formed does not respond to changes in exposure vapor isotopic composition.

These results suggest that it may be possible to discern information about the provenance and history of an oxidized U_3O_8 sample from oxygen stable isotope measurements of

metaschoepite mineral hydration water. Further work to discern the effects of exposure temperature on the oxygen stable isotope composition of metaschoepite hydration water and the durability of the signature to changes in both temperature and isotopic composition should be undertaken. Of particular interest is the relation between the oxygen isotope compositions of vapor and the incipient formation of metaschoepite on stoichiometric U_3O_8.

Data Availability

https://doi.org/10.7910/DVN/W3UKPW

Acknowledgements

We thank R. Thaw for providing the TWW water. This work was performed under the auspices of the U.S. Department of Energy by Lawrence Livermore National Laboratory under Contract DE-AC52-07NA27344, and was funded by the Office of Defense Nuclear Nonproliferation Research and Development within the U.S. Department of Energy's National Nuclear Security Administration under Project Numbers LL15-U_Surface_Oxidation-NDD3B and LL18-U Surface Oxidation Part II-NDD3Bb. Release number LLNL-JRNL-773024.

References

Bowen, G.J. (2010) Isoscapes: spatial pattern in isotopic biogeochemistry. Annual Review of Earth and Planetary Sciences 38, 161-187.

Coplen, T.B. (1994) Reporting of stable hydrogen, carbon, and oxygen isotopic abundances (technical report). Pure and Applied Chemistry 66, 273-276.

Dansgaard, W. (1964) Stable Isotopes in Precipitation. Tellus 16, 436-468.

Donald, S.B., Dai, Z.R., Davisson, M.L., Jeffries, J.R. and Nelson, A.J. (2017) An XPS study on the impact of relative humidity on the aging of UO2 powders. Journal of Nuclear Materials 487, 105-112.

Eppich, G.R., Williams, R.W., Gaffney, A.M. and Schorzman, K.C. (2013) 235 U–231 Pa age dating of uranium materials for nuclear forensic investigations. Journal of Analytical Atomic Spectrometry 28, 666-674.

Finch, R.J., Cooper, M.A., Hawthorne, F.C. and Ewing, R.C. (1996) The crystal structure of schoepite,[(UO 2) 8 O 2 (OH) 12](H 2 O) 12. The Canadian Mineralogist 34, 1071-1088.

Finch, R. J., Hawthorne, F. C., Miller, M. L., and Ewing, R. C. (1997). Distinguishing among schoepite,[(UO 2) 8 O 2 (OH) 12](H 2 O) 12, and related minerals by X-ray powder diffraction. Powder Diffraction, *12*(4), 230-238.

Finch, R.J., Hawthorne, F.C. and Ewing, R.C. (1998) Structural relations among schoepite, metaschoepite and" dehydrated schoepite". The Canadian Mineralogist 36, 831-845.

Finch, R.J., Miller, M.L. and Ewing, R.C. (1992) Weathering of natural uranyl oxide hydrates: schoepite polytypes and dehydration effects. Radiochimica Acta 58, 433-444.

Földvári, M. (2011) Handbook of thermogravimetric system of minerals and its use in geological practice. Geological Institute of Hungary Budapest.

Garrels, R.M. and Christ, C.L. (1965) Solutions, minerals, and equilibria.

He, H., Wang, P., Allred, D.D., Majewski, J., Wilkerson, M.P. and Rector, K.D. (2012) Characterization of chemical speciation in ultrathin uranium oxide layered films. Analytical chemistry 84, 10380-10387.

Horne, S., Landsberger, S. and Dickson, B. (2014) Determination of isotopic ratios of uranium samples using passive gamma spectroscopy with multiple detectors. Journal of Radioanalytical and Nuclear Chemistry 299, 1171-1175.

Keegan, E., Kristo, M.J., Colella, M., Robel, M., Williams, R., Lindvall, R., Eppich, G., Roberts, S., Borg, L. and Gaffney, A. (2014) Nuclear forensic analysis of an unknown uranium ore concentrate sample seized in a criminal investigation in Australia. Forensic science international 240, 111-121.

Kubatko, K.-A., Helean, K., Navrotsky, A. and Burns, P.C. (2006) Thermodynamics of uranyl minerals: Enthalpies of formation of uranyl oxide hydrates. American Mineralogist 91, 658-666.

Lawrence, J. and Taylor, H. (1972) Hydrogen and oxygen isotope systematics in weathering profiles. Geochimica et Cosmochimica Acta 36, 1377-1393.

Lawrence, J.R. and Taylor, H.P. (1971) Deuterium and oxygen-18 correlation: Clay minerals and hydroxides in Quaternary soils compared to meteoric waters. Geochimica et Cosmochimica Acta 35, 993-1003.

Lloyd, N.S., Mosselmans, J.F.W., Parrish, R.R., Chenery, S.R.N., Hainsworth, S.V. and Kemp, S.J. (2009) The morphologies and compositions of depleted uranium particles from an environmental case-study. De Gruyter.

Maher, K. and Chamberlain, C. (2014) Hydrologic regulation of chemical weathering and the geologic carbon cycle. Science 343, 1502-1504.

Mayer, K. (2013) Security: Expand nuclear forensics. Nature News 503, 461.

Mayer, K., Wallenius, M. and Varga, Z. (2012) Nuclear forensic science: correlating measurable material parameters to the history of nuclear material. Chemical reviews 113, 884-900.

Moody, K.J., Grant, P.M., Hutcheon, I.D. and Varoufakis, Y. (2014) Nuclear forensic analysis. CRC Press.

Oerter, E., Singleton, M. and Davisson, L. (2017) Hydrogen and oxygen stable isotope signatures of goethite hydration waters by thermogravimetry-enabled laser spectroscopy. Chemical Geology 475, 14-23.

Oerter, E.J., Singleton, M. and Davisson, M.L. (2018) Hydrogen and oxygen stable isotope dynamics of hyper-saline and salt-saturated aqueous solutions. Geochimica et Cosmochimica Acta.

Oerter, E.J., Singleton, M., Thaw, M. and Davisson, M.L. (2019) Water vapor exposure chamber for constant humidity and hydrogen and oxygen stable isotope composition. Rapid Communications in Mass Spectrometry 33, 89-96.

Plasil, J. (2018) The crystal structure of uranyl-oxide mineral schoepite, $[(UO_2)_4O(OH)_6](H_2O)_6$, revisited, Journal of Geosciences, 63, 65-73.

Savin, S.M. and Epstein, S. (1970) The oxygen and hydrogen isotope geochemistry of clay minerals. Geochimica et Cosmochimica Acta 34, 25-42.

Savin, S.M. and Hsieh, J.C. (1998) The hydrogen and oxygen isotope geochemistry of pedogenic clay minerals: principles and theoretical background. Geoderma 82, 227-253.

Sheppard, S. and Gilg, H. (1996) Stable isotope geochemistry of clay minerals. Clay Minerals 31, 1-24.

Siegel, S., H. R. Hoekstra, E. Gebert (1972) The Structure of γ-Uranyl Dihydroxide, UO2(OH)2, Acta Crystallographica, B28, 3469-3473.

Tamasi, A.L., Boland, K.S., Czerwinski, K., Ellis, J.K., Kozimor, S.A., Martin, R.L., Pugmire, A.L., Reilly, D., Scott, B.L. and Sutton, A.D. (2015) Oxidation and hydration of U3O8 materials following controlled exposure to temperature and humidity. Analytical chemistry 87, 4210-4217.